RSC Applied Interfaces

ROYAL SOCIETY OF CHEMISTRY

REVIEW

View Article Online
View Journal | View Issue

Cite this: *RSC Appl. Interfaces*, 2025, **2**, 14

Surface modification of MOFs towards flame retardant polymer composites

Xiuhong Sun,[a] Ye-Tang Pan, *[a] Wei Wang [b] and Rongjie Yang[a]

Received 12th July 2024,
Accepted 29th October 2024

DOI: 10.1039/d4lf00252k

rsc.li/RSCApplInter

Metal–organic frameworks (MOFs) have gained increasing interest as a new flame retardant material due to their high porosity, wide specific surface area, and structural flexibility. MOFs can achieve improved flame retardant qualities by modifying metal ions or adding flame retardant components to their ligands. Although MOFs' organic ligands can somewhat enhance their compatibility with the polymer matrix, their agglomeration in the matrix remains unavoidable which diminishes their effectiveness. Research indicates that surface modification of MOFs can enhance interface interactions with the polymer matrix. Consequently, modifying the surface of MOFs is crucial. Here, we categorize methods for modifying the surface structure of MOFs and examine the flame-retardant effects of various modification techniques, emphasizing the development of MOFs' surface morphology and its compatibility with the polymer matrix. In addition, we discuss the economic significance and sustainability of surface-modified MOFs compared to conventional flame retardants. Finally, we also discuss the prospects and challenges associated with this. Furthermore, we hope this work will provide a timely guide for scholars in this field and inspire future research.

1 Introduction

Metal–organic frameworks (MOFs) are a novel class of porous materials formed when metal ions and organic ligands self-assemble.[1] MOFs have attracted considerable attention in gas storage and separation, notably due to their tunable pore sizes and high specific surface areas.[2–4] Recently, researchers have begun to explore the application of MOFs in flame retardancy. In contrast to organic flame retardants (FRs), the metal components and intramolecular gaps in MOFs allow for the adsorption and catalytic decomposition of pyrolytic volatiles, thereby preventing the release of harmful gases.[5] According to numerous reports in the literature, the incorporation of MOFs as flame retardants significantly enhances the flame-retardant properties of polymers.[6] For example, Shi *et al.* found that the LOI of the composite membrane containing 1.0 wt% ZIF-8 reached 26.0%.[7] Zhang *et al.* utilized Mo-MOF as a flame retardant for EP, and the results indicated that the addition of 6.0 wt% Mo-MOF reduced the pHRR, TSP, and pCOP by 44.7%, 25.1%, and 42.9%, respectively.[8]

Although MOFs have exhibited certain flame retardant properties as fillers, their compatibility with the polymer matrix interface requires further enhancement to improve their flame retardant performance, as they tend to clump together within the polymer matrix.[9] Generally, greater hydrophobicity in flame retardants corresponds to enhanced compatibility with the polymer matrix. This enhances the uniform dispersion of flame retardants within the polymer matrix, mitigates damage to the mechanical properties of the matrix, and improves the flame retardant properties of the composite.[10] Therefore, enhancing the flame retardancy of

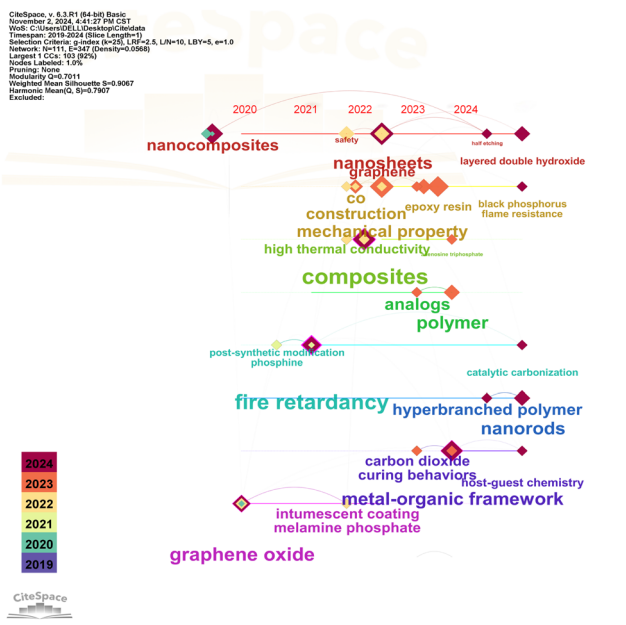

Fig. 1 Cluster analysis chart of surface modification to MOFs for flame retardant polymer composites from 2019 to 2024.

[a] *National Engineering Research Center of Flame Retardant Materials, School of Materials Science & Engineering, Beijing Institute of Technology, Beijing 100081, PR China. E-mail: pyt@bit.edu.cn*
[b] *School of Mechanical and Manufacturing, University of New South Wales, Sydney, NSW 2052, Australia*

MOFs through surface modification to increase their hydrophobicity is essential. The most common method involves introducing desired functional groups onto their surface through nanohybrids and copolymerization. For instance, to improve the dispersion of Sn-MOF in EP, PANI can be employed as a coupling agent, resulting in reductions of 42% in pHRR and 32% in THR.[11] ZIF-8-PA/PMMA composites treated with phytic acid demonstrate enhanced flame retardancy, reduced modulus, and increased hardness.[12] The improved smoke suppression effectiveness of modified ZIF-8 with α-ZrP can be attributed to their synergistic catalytic carbonization effects.[13]

Generally speaking, the surface modification of MOFs can be categorized into three primary methods: 1) hybridization of MOFs with other nanomaterials such as LDH, cyclodextrin, and MXenes; 2) polymerization of MOFs with polyphosphazene, dopamine, or similar compounds; 3) modification of surface characteristics through etching with acidic substances such as phytic acid. Fig. 1 presents the cluster analysis of MOF surface modification. The heat map intensity increases with the size of the nodes. The color becomes darker as the year progresses. These findings indicate a growing body of related research has been initiated. However, to our knowledge, no review article has been published addressing this relevant research and there is a lack of systematic classification of MOF surface modification strategies, as well as studies on their impacts on sustainable development, particularly regarding economic and environmental factors. In this study, we critically evaluate the surface modification methods of MOFs for the first time and discuss the effects of various modification techniques on the interface between flame retardants and polymers. Additionally, we assess their environmental sustainability and economic impacts. Finally, we explore the potential applications, challenges, and opportunities within this emerging field.

2 Nanohybrids

An effective approach to mitigate the agglomeration of MOFs within the polymer matrix and enhance the flame-retardant properties of polymers involves loading nanoparticles (such as MXenes, LDH, and cyclodextrin) onto MOFs to modify their surfaces. Furthermore, this method can also enhance the mechanical properties of the composite materials.[14–17] Table 1 summarizes the recently published papers on nanohybrids of MOFs and other nanomaterials.

2.1 Layered double hydroxide (LDH)

The primary components of layered double hydroxides (LDH) include interlayer anions and positively charged layers.[34] Studies indicate that the two-dimensional layered structure of LDH can release carbon dioxide and water vapor, diluting flammable gases during polymer decomposition while also impeding mass transfer between the combustion zone and the polymer matrix.[35] On the other hand, using LDH nanohybrid MOFs can effectively mitigate the agglomeration of MOFs within the polymer matrix. For example, the disparity between the internal and external stability of MOFs can serve as an *in-situ* sacrificial template to produce three-dimensional hollow LDH materials, effectively addressing the agglomeration

Table 1 Articles on hybridization of MOFs and other nanomaterials

Modifier type	Types of composite materials	Loading (wt%)	Main flame-retardant results	References
M(OH)(OCH_3)(M = Co, Ni)	EP/APTES@ZIF-67@M(OH)(OCH_3)	3.0	pHRR decreased by 20.0% The LOI value is 27.6%	18
TiO_2	EVA/TiO_2@LDHs@PANI-PA	10.0	pHRR, THR and SPR decreased by 50.9%, 43.6% and 61.9% The LOI value is 30.2%	19
GO	PLA/GPZ	2.0	pHRR decreased by 39.5% The LOI value is 27.0%	20
ATP	EVA/ZIF-67@ATP	3.0	The LOI value is 43%	21
GO	PS/GOF	1.0	pHRR and TSP decreased by 33% and 21%	14
DOPO	PLA/DOPO@Co-MOF	2.0	pHRR, SPR and pCO decreased by 27%, 56% and 20%	22
GO	PLA/ZIF-8@GO	0.5	The LOI value is 24.0%	23
α-ZrP	PUE/ZIF-8/α-ZrP	2.0	pHRR, THR, and TSP decreased by 69.6%, 45.6% and 16.6%	24
SiO_2	EP/SiO_2@UiO-66	3.0	pHRR and THR decreased by 31% and 23%	25
MoS_2	PAN/Co-Zn ZIF/MoS_2	2.0	pSPR and TSP decreased by 45.5% and 32%	26
GO	EP/MOF@GO	2.0	pHRR decreased by 30% The LOI value is 29%	27
GO	TPU/Co-ZIF-L@RGO	3.0	The LOI value is 32.6% pHRR, THR and TSP decreased by 84.4%, 70.1% and 62.5%	28
MoS_2	EP/UiO66-MoS_2	1.0	pHRR and COP decreased by 44% and 50% The LOI value is 30%	29
DOPO	BA/DOPO-NH_2-ZIF-67	2.0	pHRR and TSP decreased by 66.6% and 72.76%	30
GO	EP/ZIF-67@GO-PA	2.0	The LOI value is 29.4% pHRR and THR decreased by 57.4% and 25.7%	31
GO	TPU/APP/ZIF-67@GO	0.5	The LOI value is 27.4% pHRR and pSPR decreased by 81.2% and 48.7%	32
MoS_2	TPU/NiCo-LDH/MoS_2	2.0	pHRR and pSPR decreased by 30.9% and 55.7%	33

issue.[36] In addition to mitigating agglomeration, nanohybrids with MOFs can effectively reduce filler loading. Li *et al.* loaded ZIF-67 onto the surface of MgAl-LDH *via* electrostatic contact. Their findings revealed that 2.0 wt% of ZIF-67@MgAl-LDH reduced the pHRR and THR of EP by 62.3% and 39.9%, respectively (Fig. 2a).[37] Subsequently, RGO-LDH was synthesized by Xu *et al.* The findings indicated that 2.0 wt% RGO-LDH/ZIF-67 reduced the pHRR, THR, and TSP of EP composites by 65.7%, 35%, and 49%, respectively.[38]

Naturally inspired bionic superhydrophobic LDH/MOF hybrid materials also perform exceptionally well in mitigating the agglomeration of MOF fillers within a polymer matrix.[40] Zhou *et al.* reported a petal-shaped Co/Mg-LDH modified with APTES and BN (Fig. 2b).[39] The findings demonstrate that the FPUF nanocomposites containing 1.0 wt% BN@MOF–LDH have a rougher foam surface in their pores than pure FPUF and retain a more complete and regular micropore structure (Fig. 2c), which enhances hydrophobicity while maintaining excellent flame retardancy. MOF–LDH modified by Pio *et al.* has a bionic micro-nano composite structure that resembles lotus papillae, achieving superhydrophobic modification of flame-retardant polyurethane. Meanwhile, by serving as a co-effector in the P–N functionalized lignocellulosic fiber flame-retardant coating (LFPN), MOF–LDH endows the composites with exceptio.[41]

2.2 MXenes

MXene is a two-dimensional nanomaterial composed of transition metal carbides and nitrides, exhibiting excellent mechanical, thermal, and flame-retardant properties.[42–44] Moreover, its tunable terminations and intercalable structure facilitate the development of multifunctional MXene-based nanofillers.[45] Research indicates that modifying MXene can serve as a physical barrier, a catalyst for carbonization, and a gas-phase flame retardant. Importantly, after the modification of Co-MOF with MXene, it can also prevent the agglomeration of Co-MOF. Co-MOF@MXene is uniformly dispersed in the TPU matrix due to interactions between end-group motifs on MXene and the unsaturated sites of metal ions on the MOF. The TPU/Co-MOF@MXene composites demonstrate exceptional flame retardancy, smoke suppression, and thermal stability.[46] Three-dimensional flower-like Ni-MOFs can be functionalized with MXene ($Ti_3C_2T_x$), enhancing the dispersion of MOFs in the TPU matrix and improving the composites' flame-retardant properties (Fig. 3a).[47] Subsequently, Yu *et al.* investigated the effects of MXenes@Ni-MOFs on the flame retardancy of EP. The results indicated that the degradation of MXenes@Ni-MOFs produces metal oxides (nickel monoxide and titanium dioxide), which catalyze carbonization and promote the formation of a coating with high resistance to thermal oxidation in EP, thereby enhancing the composite's flame retardancy. The EP composite containing 2.0 wt% MXenes@Ni-MOFs exhibited reductions of 42.5%, 26.7%, and 37.7% in pTSP, pCO, and pCO_2, respectively.[48]

Gong and collaborators developed a bimetallic organic framework (Bi-MOF) with either a flaky or cubic morphology by varying the types of metal ions.[49] Observations of the fracture cross-section using scanning electron microscopy reveal that the resulting MXene@Bi-MOF/EP composite exhibits more

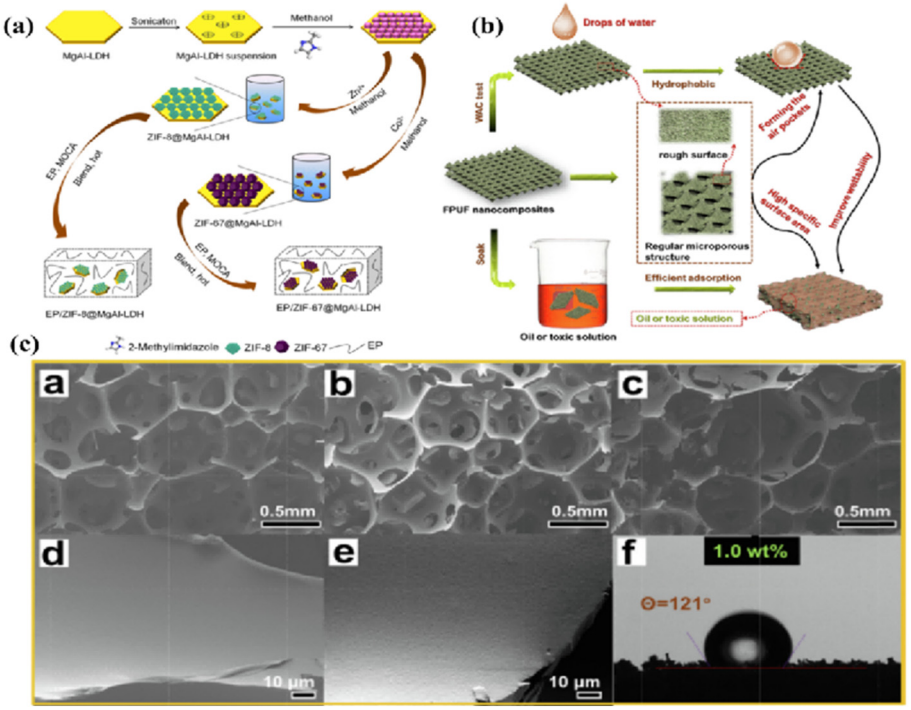

Fig. 2 (a) Diagram for modifying LDH and creating EP composites. Reproduced from ref. 37 with permission from [Elsevier], copyright [2018]; (b) oil absorption mechanism schematic diagram. Reproduced from ref. 39 with permission from [Elsevier], copyright [2022]; (c) the SEM images of a: pure FPUF, b: FPUF/BN@MOF–LDH 1.0 and c: FPUF/BN@MOF–LDH 3.0; the SEM images of d: pure FPUF and e: FPUF/BN@MOF–LDH 1.0 at high magnification; f: WAC value of FPUF/BN@MOF–LDH 1.0. Reproduced from ref. 39 with permission from [Elsevier], copyright [2022].

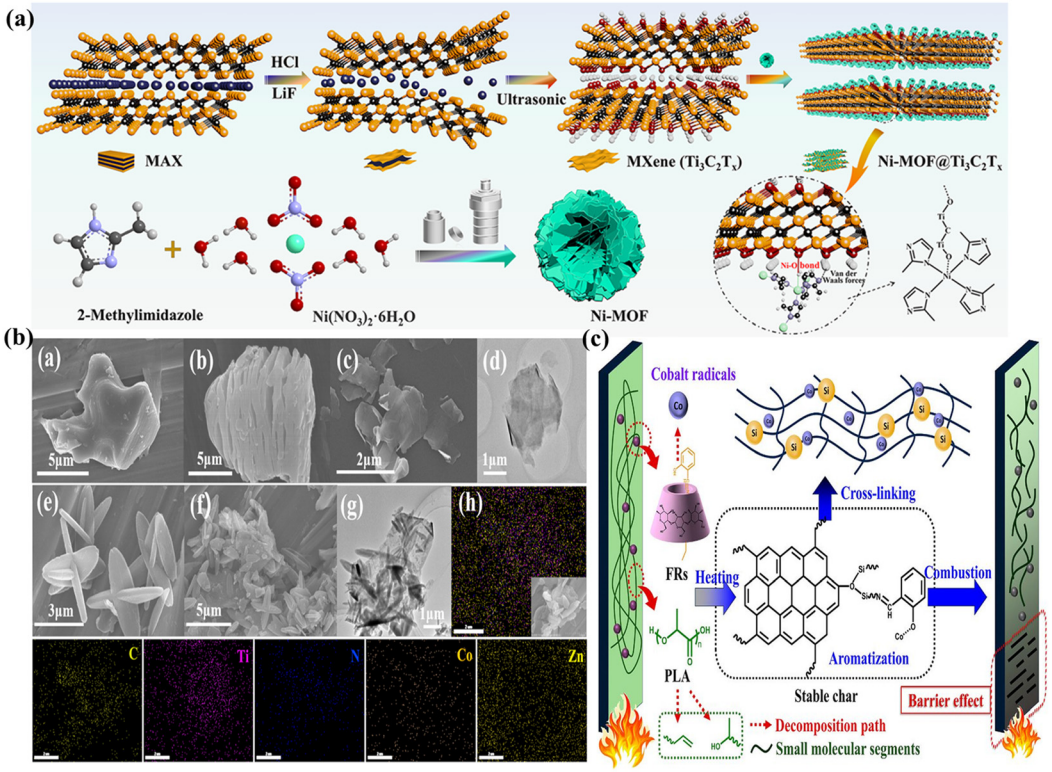

Fig. 3 (a) Diagram for the synthetic Ni-MOF@$Ti_3C_2T_x$ pathway. Reproduced from ref. 47 with permission from [Elsevier], copyright [2022]; (b) SEM images of MAX precursor (a), m-MXene (b), MXene nanosheets (c), Bi-MOF (e) and MXene@Bi-MOF hybrids (f); TEM images of MXene nanosheets (d) and MXene@Bi-MOF hybrids (g); EDS images of MXene@Bi-MOF hybrids (h). Reproduced from ref. 49 with permission from [Elsevier], copyright [2022]; (c) a proposed strategy for PLA/5βCD-MOF@Schiff base composites to prevent fire. Reproduced from ref. 50 with permission from [Elsevier], copyright [2024].

dimensional cracks, a rougher surface, and a lack of discernible polymerization. This is attributed to the loading of Bi-MOF onto the MXene surface, which facilitates the hybrid's dispersion within the matrix and enhances its compatibility with the polymer. The way it works is that MXene@Bi-MOF can function as a multilayered barrier to stop heat and smoke from escaping. The gas-phase dilution effect of Bi-MOF further contributes to the enhanced fire safety of EP composites (Fig. 3b). Then, the results indicate that selective laser sintering technology enhances the uniform distribution of MXene-1 on HKUST within the PA12 matrix. This improvement is primarily attributed to the increased melt viscosity of the PA12/MHK composite powder, which facilitates better mixing between the filler and the matrix.[51]

2.3 β-Cyclodextrin (β-CD)

The hydrophobic inner ring and outer hydroxyl groups of β-CD facilitate intramolecular interactions.[52] Leveraging this property, our team developed a tri-functional host-guest flame retardant based on β-CD (βCD-MOF@Schiff base) by self-crosslinking the Schiff base within the β-CD cavity and incorporating MOFs onto its surface.[50] Data indicate that the β-CD modified by MOFs has reduced to a particle size of 8–10 μm and has assumed an irregular spherical shape. This may result from ongoing recrystallization during the synthesis process.[53] After compounding the βCD-MOF@Schiff base with PLA, the composite exhibited an LOI value of 29%, and the THR decreased by 17%. This can be attributed to the βCD-MOF@Schiff alkali flame retardant's ability to decompose cobalt-containing free radicals at various temperatures, promoting the formation of a carbon phase and creating a physical barrier with a high degree of graphitization (Fig. 3c).

2.4 Graphite carbon nitride (g-C_3N_4)

g-C_3N_4 is a two-dimensional layered structure that effectively applies the physical barrier effect and reduces the rate of heat deterioration in composites.[54,55] Additionally, the –NH_2 and –NH hydrophilic groups of g-C_3N_4 can serve as doping and grafting sites in small quantities, enabling the formation of a Bi-MOF/g-C_3N_4 mixed flame retardant with an enhanced nano-polymer interface.[56] For instance, Yang *et al.* employed a co-precipitation technique to deposit g-C_3N_4 onto the surface of CoCu-MOF, significantly enhancing the hydrophobicity of the resulting BMCN.[57] This improvement is primarily attributed to the presence of organic bonds in CoCu-MOF, the complexation of g-C_3N_4 with metal ions, and the increased surface roughness of BMCN. Due to its enhanced hydrophobicity, BMCN exhibits better distribution

and stability in UPR. Moreover, BMCN promotes the formation of a thick carbon layer in UPR, inhibiting the emission of hazardous gases. The results indicated that the pHRR, pSPR, pCO, and PTSP decreased by 43.4%, 50.0%, 79.6%, and 32.5%, respectively, upon the introduction of only 4.0 wt% BMCN.

3 Polymerization

By meticulously controlling the reaction conditions and incorporating phosphorus-containing and nitrogen-containing compounds, such as polyphosphazene and dopamine, with MOFs, the surface structure of the copolymer can be modified, thereby altering the interface between the polymer and the filler.[58] Consequently, the flame-retardant properties of polymer nanocomposites are anticipated to vary under different interface conditions. Table 2 summarizes the papers on the surface modification of MOFs using nanomaterials *via* polymerization.

3.1 Polyphosphazene (PZS)

Polyphosphazene (PZS) consists of side chains with various organic substituents and a core chain featuring alternating nitrogen and phosphorus atoms.[66] By introducing specific groups, PZS can enhance compatibility with the matrix and simultaneously undergo copolymerization with other flame retardants, resulting in exceptional flame-retardant properties. This capability is facilitated by the designability of its side groups. For example, the incorporation of amino groups into PZS allows it to function as an interfacial compatibilizer and flame retardant, enabling the design and synthesis of a three-dimensional NiCo-LDH@PZS with a hollow dodecahedron structure. Results indicate that NiCo-LDH@PZS possesses a rougher surface and a hollow polyhedral shape, enhancing its compatibility with the polymer matrix. Furthermore, it effectively enhances the flame retardancy of EP while preventing the release of toxic smoke[67] (Fig. 4a). Subsequently, PZS was applied to the surface of Fe-MOF. Electron microscopy results demonstrated that PZS effectively coated the exterior of Fe-MOF, enhancing interfacial compatibility between EP and Fe-MOF. The synergistic flame-retardant properties of these materials promote the formation of a dense carbon layer, thereby safeguarding the EP substrate and limiting smoke emissions. The findings indicate that the pHRR, THR, SPR, and TSP of the EP/3.0 wt% PZS-Fe-MOF composites decreased by 30.2%, 36.9%, 36.6%, and 41.4%, respectively.[68]

More significantly, a well-dispersed filler within the polymer matrix can enhance both the mechanical properties of materials and the flame-retardant performance of composites. Through covalent bonds and physical adsorption, Lv *et al.* synthesized ZIF-8@PZN by growing PZN on the surface of ZIF-8. The network structure of the –P–N– bonds in PZN and the presence of amino reactive groups significantly enhance the compatibility and interfacial interaction between ZIF-8@PZN and EP.[59] As a result, the pHRR of the EP/ZIF-8@PZN3.0 composites was significantly reduced by 49.8%, while their σ and E increased to 77.9 ± 2.8 MPa and 4183 ± 82.5 MPa, respectively. To customize the interface of polymer nanocomposites more accurately and explore the interface interaction of different hybrids, our group developed LDH@PZS@NH and ZIF@LDH@PZS with varied outer layers[69] (Fig. 4b). As a result, the hybrid's different outer layers gave them different interfacial interactions (Table 3). The interfacial energy of EP/ZIF@LDH@PZS is lower than that of EP/LDH@PZS@NH, which makes the dispersion degree of ZIF@LDH@PZS particles in EP better than that of LDH@PZS@NH. Thus, ZIF@LDH@PZS has outstanding flame retardant performance.

3.2 Polydopamine (PDA)

Numerous studies indicate that poly-dopamine (PDA) can self-polymerize to deposit on various inorganic and organic surfaces, providing a practical approach for the surface modification of MOFs. Utilizing PDA as a linker, Zhang *et al.* developed UiO66-PDA–PBA, which exhibits a flower-like morphology.[70] The tailored layered structure of UiO66-PDA–PBA allows it to uniformly disperse within the EP matrix, generating an interfacial catalytic effect that enhances flame retardant efficiency. Also using PDA as a linker, chen and colleagues linked ATP with BN and anchored Cu-MOF nanoparticles uniformly on its surface.[71] The findings demonstrate that the BN/PATP@Cu-MOF has good dispersibility in EP resin. Simultaneously, through the synergistic effect of ATP, BN and Cu-MOF, the

Table 2 Articles on the surface modification of MOFs using nanomaterials *via* polymerization

Modifier type	Types of composite materials	Loading (wt%)	Main flame-retardant results	References
PZN	EP/ZIF-8@PZN/APP	3.0	pHRR and pSPR decreased by 80.8% and 72.6% respectively	59
PANI	PUA/PANI@Co-PA-2.0	5.0	pHRR and THR decreased by 54.9% and 59.9%	60
PCT	PS/PCT@MOF-NH_2	3.0	pHRR and THR decreased by 40% and 31%	61
APP	EP/ZIF-8@APP	5.0	pHRR and THR decreased by 60.8% and 35.5% respectively	62
APP	Wood/APz@ZIF67	10.0	The LOI value is 48.55% TSP decreased by 43.78%	63
APP	UPR/APP@UiO	10.0	pHRR and SPR decreased by 61.34% and 37.5% The LOI value is 31.2%	64
APP	TPU/APP@MOFs	20.0	pHRR, THR, SPR, TSP, YCO and YCO_2 decreased by 75.76%, 86.19%, 69.74%, 86.34%, 57.14% and 76.37% respectively	65

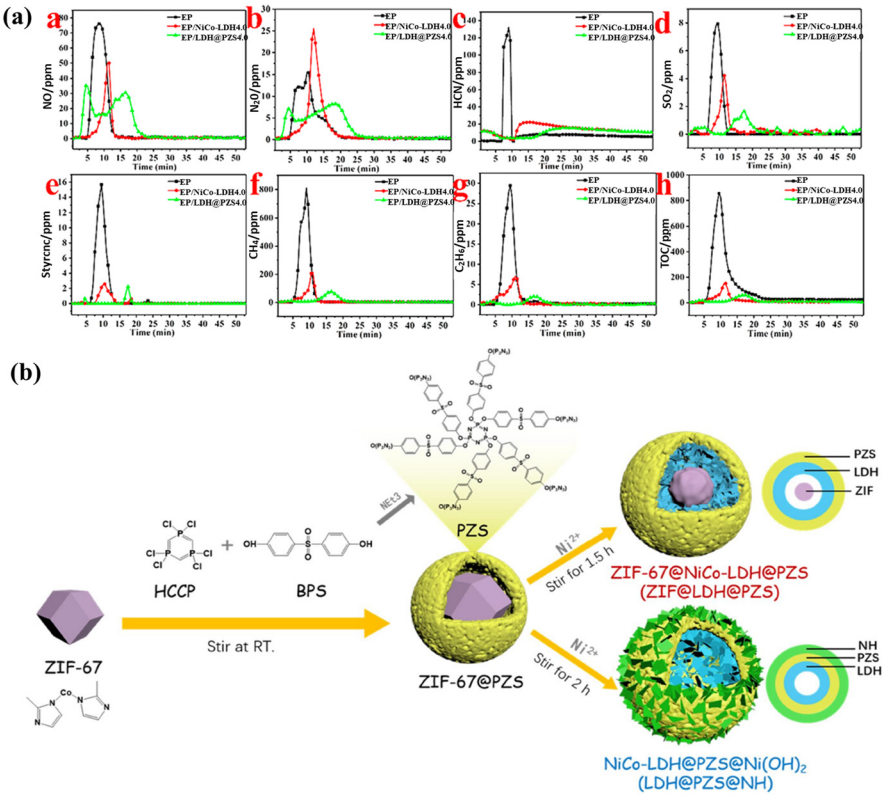

Fig. 4 (a) Time curves showing the generation of harmful gases during combustion (a–h) for pure EP, EP/NiCo-LDH 4.0, and EP/NiCo-LDH@PZS 4.0. Reproduced from ref. 67 with permission from [American Chemical Society], copyright [2019]; (b) diagrammatic representation of the synthetic pathways for two samples with distinct nanostructures. Reproduced from ref. 69 with permission from [American Chemical Society], copyright [2022].

composite material forms an expanded carbon network with greater strength and barrier performance, which greatly reduces the TSP and THR. The flame retardancy of RPUF can also be greatly increased by APP@PDA-ZIF-67 (A@P-Z), according to reports by Liu and others, the uniform embedding of ZIF-67 on the surface of A@P is one of the causes, since it greatly boosts the filler's specific surface area and matrix compatibility.[72]

To further improve the compatibility between resin matrix and LDH through PDA. Our group used PDA to modify ZIF-67 to create TPP@LDH@Co–PDA.[73] Due to the formation of coordination bonds between nitrogen and metal ions, the hybrid has less surface polarity and surface energy. EP/TPP@LDH@Co–PDA exhibits high compatibility and interface interaction (Fig. 5a). Simultaneously, due to a Co–P–N ternary flame retardant system was successfully created, the composite material's pHRR (43.1%) decreased with 2.0 wt% TPP@LDH@Co–PDA.

4 Acid etching

Utilizing phosphorus-rich materials to etch the surfaces of MOFs is an effective strategy to enhance the flame retardant efficiency that is often limited when using MOFs alone. Among various phosphorus-containing flame retardants, phytic acid (PA) is a biocompatible organic acid that is environmentally safe and has garnered increasing attention. Zhang *et al.* modified UiO66-NH_2 with PA to synthesize PA–UiO66-NH_2. The –NH_2 functionalized MOFs exhibit strong interfacial compatibility with polymers, thereby enhancing the interfacial strength of the composites and providing effective flame retardancy.[76] Building on this, the use of β-CD as an additional carbon source, combined with the synergistic effect of PA–UiO66-NH_2, facilitated the formation of an expanded carbon layer. Consequently, the pHRR of the EP/β-CD@P-MOF samples decreased by 53%.[77]

Table 3 Contact angle data and surface energy results for EP and hybrids. Reproduced from ref. 69 with permission from American Chemical Society

Sample	Contact angle (degrees)		γ^{d}_{SV} (MJ m^{-2})	γ^{p}_{SV} (MJ m^{-2})	γ_{SV} (MJ m^{-2})	γ_{12} (MJ m^{-2})
	θ_{water}	$\theta_{CH_2I_2}$				
EP	105.6 ± 1.0	60.3 ± 0.5	29.4	0.04	29.8	—
ZIF@LDH@PZS	70.6 ± 0.5	71.3 ± 2.0	14.9	17.1	32.0	18.4
LDH@PZS@NH	51.8 ± 1.0	40.1 ± 0.5	28.9	21.8	50.7	20.7

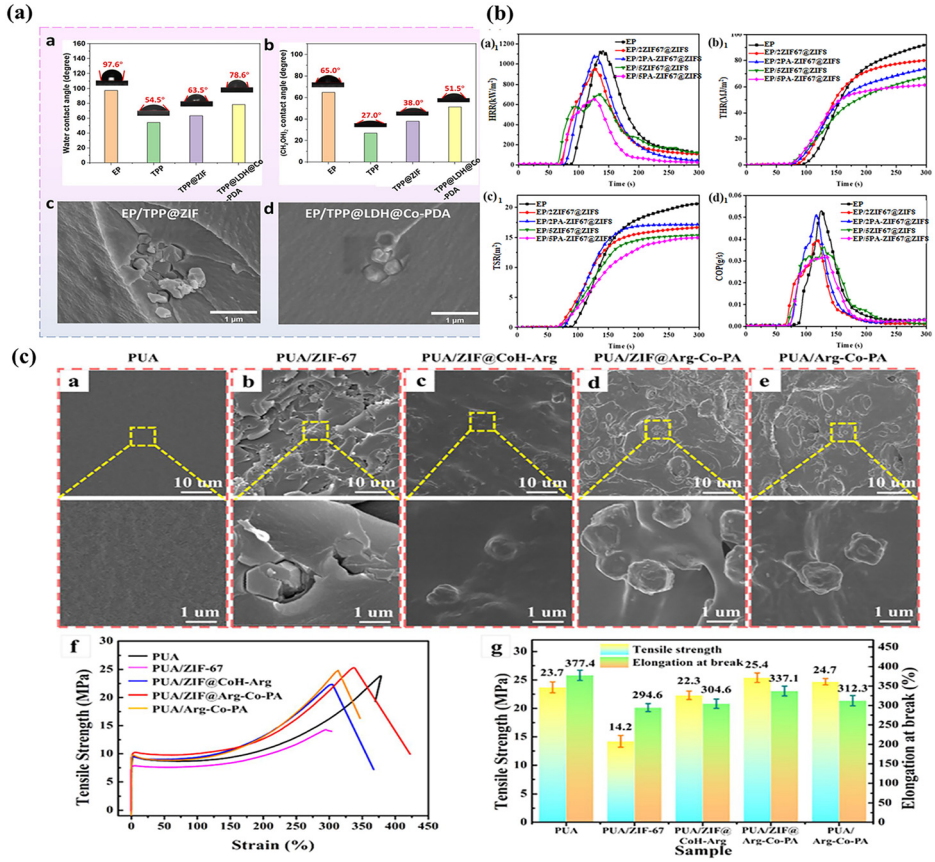

Fig. 5 (a): Contact angles for EP, TPP, TPP@ZIF, and TPP@LDH@Co–PDA in water and ethylene glycol (a and b); SEM pictures of the fracture surfaces of (c) EP/TPP@ZIF and (d) EP/TPP@LDH@Co–PDA. Reproduced from ref. 73 with permission from [Elsevier], copyright [2024]; (b): (a_1) HRR, (b_1) THP, (c_1) TSP, and (d_1) COP curves of EP and its composites. Reproduced from ref. 74 with permission from [American Chemical Society], copyright [2022]; (c): (a–e) SEM pictures of the broken surface for PUA and its composites, as well as magnified SEM images. (f) Stress–strain profiles and (g) the tensile strength and elongation at break histogram of PUA and its composites. Reproduced from ref. 75 with permission from [American Chemical Society], copyright [2024].

ZIF-8 is a type of MOF composed of Zn^{2+} and P. Surface modification with phytic acid (PA) results in enhanced non-covalent interactions and a more effective carbon barrier.[12] Consequently, PA/ZIF-8 can be utilized to prepare PMMA composites that exhibit superior mechanical and fire safety properties. To further enhance flame retardant efficiency, Wang *et al.* synthesized ZIF-67@ZIF-8 with a core–shell structure, which was subsequently functionalized with PA.[74] The results indicated that the TSP, pHRR, and pCOP of the composites decreased significantly by 27.2%, 42.2%, and 41.5%, respectively, following the addition of 5.0 wt% ZIF-67@ZIF-8-PA. This improvement was primarily due to the synergistic flame retardant effects of the various components (Fig. 5b).

However, the phenomenon of over-etching frequently occurs during the modification of MOFs with PAs. To address this issue, our group proposed to form a buffer layer on the periphery of ZIF-67 through the weak etching of alkali arginine.[75] The ZIF@Arg–Co–PA obtained by this strategy protects the pore characteristics of ZIF-67, exposes more active sites, enhances the interaction with the polymer matrix, and helps to improve the comprehensive properties of polyurea composites. Under the load of only 5.0 wt%, ZIF@Arg–Co–PA made the LOI value of polyurea composites reach 23.2%, and pHRR, THR, and TSP decreased by 43.8%, 32.3%, and 34.3% respectively. Meanwhile, there has been a range of improvement in the mechanical characteristics of the composites (Fig. 5c).

5 Assessment of the economy and environmental advantages of surface-modified MOFs

5.1 Advantages for the environment

The development of sustainable materials has emerged as a prominent topic in the materials industry, serving as a strategy to combat global environmental degradation.[78] Due to their high specific surface area and porous structure, MOFs inherently outperform conventional organic and inorganic flame retardants in smoke absorption. This characteristic contributes to environmental protection by diminishing the emission of harmful smoke from materials. Moreover, the structural adaptability of MOFs is a significant advantage.[79] This adaptability ensures the flame retardancy of MOFs and

facilitates their biodegradability, achieved through etching with biomass acids or incorporating biological regulators into their ligands to modify their surface properties.[80]

Phytic acid is a biocompatible and environmentally friendly organic acid that is commonly utilized to modify flame retardants (FRs) owing to its high phosphorus content (28% P).[74] β-Cyclodextrin, derived from starch and polysaccharides, can reduce the toxicity and low melting point associated with phosphorus-containing flame retardants. Both substances modify metal–organic frameworks (β-CD@P-MOF), which are uniformly dispersed in epoxy resin, significantly enhancing the mechanical properties of the composites (Fig. 6a). Furthermore, β-CD@P-MOF contains numerous phosphate and amino groups that can serve as sources of gas and acid. This facilitates the formation of expanded carbon and reduces the pHRR and SPR of the composites by 41% and 62%, respectively.[77] Similar optimal results can be achieved with other biomass regulators, such as polydopamine and o-vanillin. For example, Xue *et al.* synthesized a bio-MOF (ZIF-oV) by coordinating with Zn^{2+} and generating the biobased organic ligand oVBZMI from o-vanillin. It was found that the interfacial interaction between ZIF-oV and EP was enhanced by oVBZMI, which possesses nitrogen-containing functional groups. This improvement resulted in enhanced mechanical properties of the materials and effectively reduced the pHRR of EP by approximately 50%.[81]

Moreover, surface-modified MOFs show considerable potential as versatile fillers for direct application in environmental remediation.[84] By incorporating suitable modifiers, MOFs effectively function as both flame retardants and oil–water separators, thereby fulfilling dual roles in sewage treatment. For example, applying copper–benzenedicarboxylic acid (Cu–BDC) MOF as a flame retardant and incorporating nano-graphite flakes (NGPs) as a superhydrophobic agent onto the surface of polyurethane sponge can significantly reduce the surface energy of the MF and enhance the uniform dispersion of fillers within the matrix. Experimental results indicate that the PU–Cu(BDC)–NGP composite exhibits an oleophilic and superhydrophobic contact angle of approximately 154°. This composite achieves effective oil–water separation, evidenced by a LOI value of 24.46%.[85] Likewise, when UiO-66 is modified with octadecylphosphonic acid (OPA), it can achieve superhydrophobic and flame retardant properties in melamine foam (MF) sponge, with a contact angle reaching approximately 172.3°, thus enabling its application in sewage treatment (Fig. 6b).[82]

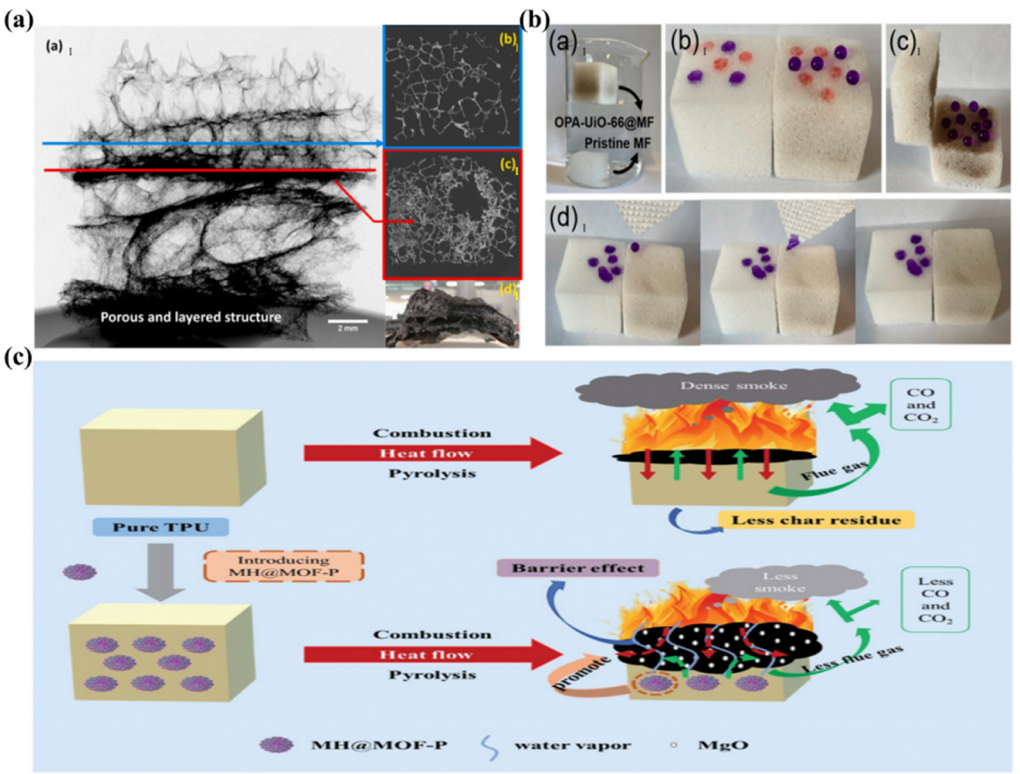

Fig. 6 (a): Results of X-ray tomography of EP composites with 7% βCD@P-MOF (a_1), with the selected layer at loose (b_1) and accumulated (c_1), digital photo of the cross-section view of the cut char residue (d_1). Reproduced from ref. 75 with permission from [Elsevier], copyright [2021]; (b): (a_1) MF sponge and OPA-UiO-66@MF in water; (b_1) *n*-hexane (red dyed) and water (purple dyed) droplets on MF sponge (left) and OPA-UiO-66@MF (right); (c_1) the wetting behaviors of the water droplets on the cross section of OPA-UiO-66@MF; (d_1) the wetting behaviors of the droplets on MF sponge and OPA-UiO-66@MF. Reproduced from ref. 82 with permission from [Elsevier], copyright [2022]; (c): Schematic illustration for flame retardant mechanism of TPU composites with MOF@MH–P. Reproduced from ref. 83 with permission from [The Royal Society of Chemistry], copyright [2021].

5.2 Advantages for the economic

After surface modification, MOFs also show attractive prospects in terms of economic benefits. As previously discussed, whether through surface hybrid modification, copolymerization modification, or acid etching, it has significantly contributed to the enhancement of flame retardancy and the mitigation of economic losses resulting from fire.[86] In addition, surface-modified MOFs positively contribute to lowering filler content and consequently reducing costs, and their industrial applications exhibit substantial developmental potential.[87] Furthermore, modified phosphorus tailings, the residual solid waste from phosphate rock, can be transformed into MH@MOF through the application of MOFs. This substance has the ability to adsorb and extract phosphate that is abundant in water. Furthermore, studies have revealed that the hybrid MH@MOF and polymer matrix exhibit markedly improved compatibility, and the composite material MH@MOF–P, following phosphate adsorption, may serve as an effective flame retardant for TPU (Fig. 6c).[83] In addition to recovering and processing phosphorus tailings and mitigating water eutrophication, this approach can also utilize the recovered materials to produce TPU flame retardants, thereby conserving natural resources and enhancing the profitability of phosphate rock treatment facilities. This also provides valuable insights for the industrial treatment of phosphorus tailings.

Conclusions

Based on the above reports about the surface modification of MOFs, we present a concise summary here. (1) The surface modification of MOFs primarily encompasses nanohybrids, polymerization, and acid etching; (2) hybridization of MOFs with nanoparticles such as MXenes, LDH, and cyclodextrin can significantly enhance the dispersion of flame retardants (FRs) in the polymer matrix, contributing to a synergistic flame-retardant effect and improving flame retardant efficiency; (3) polyphosphazene, dopamine, and other nitrogen- and phosphorus-containing chemicals can modify the surface structure of the hybrid. Selecting an appropriate copolymer can effectively improve the interfacial compatibility between the hybrid and the matrix; (4) by using phytic acid to erode the surface of MOFs, a multifunctional composite with superior flame retardancy can be developed. Furthermore, choosing certain biological modifiers can enhance the compatibility of fillers with the polymer matrix while also promoting sustainable development. MOFs can also be converted into multipurpose sewage treatment fillers with the right modifiers, providing strategic direction for the industry while enhancing economic benefits.

Although significant progress has been made in the research on the surface modification of MOFs for flame retardancy, there remains a gap between research and industrial application, necessitating further research and resolution.

(1) Despite the availability of some commercial MOFs, the costs associated with flame retardants derived from the surface modification of MOFs remain high, highlighting the need to identify effective strategies for cost reduction.

(2) The interface control between MOFs and the polymer matrix can be achieved through the modification of MOF interfaces to customize the interfaces of polymer nanocomposites. However, most methods are complex and lack precise control, requiring further simplification.

(3) Based on the surface modification of MOFs, there is still a lot of work to be done to develop multifunctional MOF composites with excellent flame retardancy.

Data availability

No primary research results, software or code have been included and no new data were generated or analysed as part of this review.

Author contributions

Xiuhong Sun: writing – original draft, data curation. Ye-Tang Pan: writing – review & editing, project administration, investigation. Wei Wang: writing – review & editing. Rongjie Yang: methodology, supervision.

Conflicts of interest

There are no conflicts to declare.

Acknowledgements

This work was supported by the National Natural Science Foundation of China (No. 22375023, 22005029), Natural Science Foundation of Chongqing (CSTB2024NSCQ-MSX0452), and Natural Science Foundation of Hebei Province (E2024105006).

Notes and references

1 Y. Hou, W. Hu, Z. Gui and Y. Hu, *Compos. Sci. Technol.*, 2017, **152**, 231–242.
2 Y. Zheng, Y. Lu and K. Zhou, *J. Therm. Anal. Calorim.*, 2019, **138**, 905–914.
3 K. Song, X. Bi, C. Yu, Y.-T. Pan, H. Vahabi, V. Realinho, J. He and R. Yang, *ACS Appl. Mater. Interfaces*, 2024, **16**, 7617–7630.
4 X. Bi, K. Song, H. Zhang, Y.-T. Pan, J. He, D.-Y. Wang and R. Yang, *Chem. Eng. J.*, 2024, **482**, 148997.
5 R. Huang, X. Guo, S. Ma, J. Xie, J. Xu and J. Ma, *Polymer*, 2020, **12**, 108.
6 M. Zhang, Y. Gao, Y. Zhan, X. Ding, M. Wang and X. Wang, *Materials*, 2018, **11**, 1756.
7 X. Shi, X. Dai, Y. Cao, J. Li, C. Huo and X. Wang, *Ind. Eng. Chem. Res.*, 2017, **56**, 3887–3894.
8 F. Zhang, X. Li, L. Yang, Y. Zhang and M. Zhang, *Polym. Adv. Technol.*, 2021, **32**, 3266–3277.
9 K. Song, Y.-T. Pan, J. He and R. Yang, *Ind. Chem. Mater.*, 2024, DOI: **10.1039/d3im00110e**.

10 Y. Hou, Z. Xu, Y. Yuan, L. Liu, S. Ma, W. Wang, Y. Hu, W. Hu and Z. Gui, *Compos. Sci. Technol.*, 2019, **177**, 66–72.
11 S. Ma, Y. Hou, Y. Xiao, F. Chu, T. Cai, W. Hu and Y. Hu, *Mater. Chem. Phys.*, 2020, **247**, 122875.
12 L. Wang, X. Hu, Z. Mao, J. Wang and X. Wang, *Polymer*, 2022, **14**, 4871.
13 B. Hou, Y.-T. Pan and P. Song, *Microstructures*, 2023, **3**, 300039.
14 Y. Hou, W. Hu, X. Zhou, Z. Gui and Y. Hu, *Ind. Eng. Chem. Res.*, 2017, **56**, 8778–8786.
15 K. Song, Y.-T. Pan, J. Zhang, P. Song, J. He, D.-Y. Wang and R. Yang, *Chem. Eng. J.*, 2023, **468**, 143653.
16 S. Mandal, D. Roy, K. Mukhopadhyay, M. Dwivedi and M. Joshi, *RSC Appl. Interfaces*, 2024, **1**, 977–991.
17 W. Xu, G. Wang, J. Xu, Y. Liu, R. Chen and H. Yan, *J. Hazard. Mater.*, 2019, **379**, 120819.
18 X. Dong, D.-L. Li, L. Xie, X. Fan and Y.-X. Feng, *J. Polym. Res.*, 2024, **31**, 40.
19 L. Wang, W.-J. Yan, C.-Z. Zhong, C.-R. Chen, Q. Luo, Y.-T. Pan, Z.-H. Tang and S. Xu, *Mater. Today Chem.*, 2024, **36**, 101952.
20 M. Zhang, X. Ding, Y. Zhan, Y. Wang and X. Wang, *J. Hazard. Mater.*, 2020, **384**, 121260.
21 D.-X. Ma, Y. Yang, G.-Z. Yin, A. Vázquez-López, Y. Jiang, N. Wang and D.-Y. Wang, *Polymer*, 2022, **14**, 4408.
22 Y. Hou, L. Liu, S. Qiu, X. Zhou, Z. Gui and Y. Hu, *ACS Appl. Mater. Interfaces*, 2018, **10**, 8274–8286.
23 M. Zhang, X. Shi, X. Dai, C. Huo, J. Xie, X. Li and X. Wang, *J. Mater. Sci.*, 2018, **53**, 7083–7093.
24 B. Xu, W. Xu, Y. Liu, R. Chen, W. Li, Y. Wu and Z. Yang, *Polym. Adv. Technol.*, 2018, **29**, 2816–2826.
25 W. Guo, S. Nie, E. N. Kalali, X. Wang, W. Wang, W. Cai, L. Song and Y. Hu, *Composites, Part B*, 2019, **176**, 107261.
26 H. Peng, L. Zhang, M. Li, M. Liu, C. Wang, D. Wang and S. Fu, *Chem. Eng. J.*, 2020, **397**, 125410.
27 J. Zhang, Z. Li, X. Qi, W. Zhang and D.-Y. Wang, *Composites, Part B*, 2020, **188**, 107881.
28 W. Xu, C. Cheng, Z. Qin, D. Zhong, Z. Cheng and Q. Zhang, *Polym. Adv. Technol.*, 2020, **32**, 228–240.
29 J. Zhang, X. Ao, X. Zhang, R. Wang, X. Jin, W. Ye, B. Xu and D.-Y. Wang, *ACS Appl. Nano Mater.*, 2022, **5**, 17731–17740.
30 J. Yang, A. Zhang, Y. Chen, L. Wang, M. Li, H. Yang and Y. Hou, *Chem. Eng. J.*, 2022, **430**, 132809.
31 H. Wang, Z. He, X. Li, Y. Wang, D. Yao and Y. Zheng, *J. Appl. Polym. Sci.*, 2022, **139**, e52211.
32 Q. Liu, H. Wang, H. Li, J. Sun, X. Gu and S. Zhang, *Polym. Adv. Technol.*, 2022, **33**, 2374–2385.
33 Y. Qian, W. Su, L. Li, R. Zhao, H. Fu, J. Li, P. Zhang, Q. Guo and J. Ma, *Polymer*, 2022, **14**, 2204.
34 G. Prestopino, R. Pezzilli, N. J. Calavita, C. Leonardi, C. Falconi and P. G. Medaglia, *Nano Energy*, 2023, **118**, 109017.
35 C. Deng, Y. Liu, H. Jian, Y. Liang, M. Wen, J. Shi and H. Park, *Constr. Build. Mater.*, 2023, **374**, 130939.
36 Z. Zhang, X. Li, Y. Yuan, Y. T. Pan, D. Y. Wang and R. Yang, *ACS Appl. Mater. Interfaces*, 2019, **11**, 40951–40960.
37 A. Li, W. Xu, R. Chen, Y. Liu and W. Li, *Composites, Part A*, 2018, **112**, 558–571.
38 W. Xu, X. Wang, Y. Liu, W. Li and R. Chen, *Polym. Degrad. Stab.*, 2018, **154**, 27–36.
39 Y. Zhou, S. Qiu, F. Chu, W. Yang, Y. Qiu, L. Qian, W. Hu and L. Song, *J. Colloid Interface Sci.*, 2022, **609**, 794–806.
40 Y.-T. Pan, Z. Zhang and R. Yang, *Composites, Part B*, 2020, **199**, 108265.
41 J. Piao, M. Lu, J. Ren, Y. Wang, T. Feng, Y. Wang, C. Jiao, X. Chen and S. Kuang, *J. Hazard. Mater.*, 2023, **444**, 130398.
42 W. Wang, C. Wang, A. C. Y. Yuen, A. Li, B. Lin, Y. Yuan, C. Ma, Y. Han and G. H. Yeoh, *Composites, Part A*, 2023, **173**, 107673.
43 L. Zhang, L. Nie, S. Zhang, Z. Dong, Q. Zhou, Z. Zhang and G.-B. Pan, *Mater. Lett.*, 2022, **314**, 131820.
44 J. Su, Q. Ma, L. Que, H. Jiang, X. Xu, Y. Wang, Y. Guo and Z. Zhou, *Nano Res.*, 2023, **16**, 6369–6379.
45 S. K. Raj, V. Sharma, S. Mishra and V. Kulshrestha, *RSC Appl. Interfaces*, 2024, **1**, 1057–1068.
46 C. Shi, M. Wan, Z. Hou, X. Qian, H. Che, Y. Qin, J. Jing, J. Li, F. Ren, B. Yu and N. Hong, *Polym. Degrad. Stab.*, 2022, **204**, 110119.
47 M. Wan, C. Shi, X. Qian, Y. Qin, J. Jing, H. Che, F. Ren, J. Li and B. Yu, *Composites, Part A*, 2022, **163**, 107187.
48 S. Yu, C. Cheng, K. Li, J. Wang, Z. Wang, H. Zhou, W. Wang, Y. Zhang and Y. Quan, *Chem. Eng. J.*, 2023, **465**, 143039.
49 K. Gong, L. Cai, C. Shi, F. Gao, L. Yin, X. Qian and K. Zhou, *Composites, Part A*, 2022, **161**, 107109.
50 J. Zhang, X. Zhang, R. Wang, W. Wang, H. Zhao, S. Yang, Z. Dong, D.-Y. Wang and Y.-T. Pan, *Carbohydr. Polym.*, 2024, **341**, 122313.
51 L. Chen, B. Huang, F. Wei, X. Guo, D. Zhang, K. Thummavichai, D. Chen, N. Wang and Y. Zhu, *ACS Appl. Polym. Mater.*, 2023, **5**, 9852–9864.
52 N. Zhang, E. Yildirim, C. P. Zane, J. Shen, N. Vinueza, D. Hinks, A. E. Tonelli and M. A. Pasquinelli, *ACS Appl. Polym. Mater.*, 2019, **1**, 2768–2777.
53 Q. Li, Z. Han, X. Song, Y.-T. Pan, Z. Geng, H. Vahabi, V. Realinho and R. Yang, *Carbohydr. Polym.*, 2024, **333**, 121980.
54 Z. Chen, Y. Suo, Y. Yu, T. Chen, C. Li, Q. Zhang, J. Jiang and T. Chen, *Compos. Commun.*, 2022, **29**, 101018.
55 H. Shivakumar, G. D. Gurumurthy, K. B. Bommegowda and S. Parameshwara, *J. Polym. Mater.*, 2023, **40**, 93–103.
56 W. Zhang, W. Wu, W. Meng, W. Xie, Y. Cui, J. Xu and H. Qu, *Polymer*, 2020, **12**, 212.
57 B. Yang, Z. Chen, Y. Yu, T. Chen, Y. Chu, N. Song, Q. Zhang, Z. Liu, Z. Liu and J. Jiang, *Mater. Today Chem.*, 2023, **30**, 101482.
58 A. Munni, M. A. Bashammakh, M. Bellier, A. Ansari, M. E. A. Ali, H. E. Karahan, R. Islam, T. H. Boyer and F. Perreault, *RSC Appl. Interfaces*, 2024, DOI: **10.1039/d4lf00088a**.
59 X. Lv, W. Zeng, Z. Yang, Y. Yang, Y. Wang, Z. Lei, J. Liu and D. Chen, *Polym. Adv. Technol.*, 2020, **31**, 997–1006.
60 X. Bi, K. Song, Y. T. Pan, C. Barreneche, H. Vahabi, J. He and R. Yang, *Small*, 2023, **20**, 2307492.
61 Z. Xu, W. Xing, Y. Hou, B. Zou, L. Han, W. Hu and Y. Hu, *Combust. Flame*, 2021, **226**, 108–116.

62 Z. Yue, J. Lin, D. Yang, Y. Zhu, J. Li, J. Zhou and X. Wang, *J. Mater. Sci.*, 2022, **57**, 20082–20094.
63 F. Tian, Y. Wu, C. Zhu, Y. She, Y. Jin, B. Wang, H. Chen, H. Xu, Y. Liu, S. Wang and X. Xu, *Chem. Eng. J.*, 2024, **483**, 149393.
64 J. Du, X. Fan, F. Xin, Y. Chen, K. Feng and J. Hu, *Eur. Polym. J.*, 2024, **207**, 112820.
65 C. Shi, M. Wan, X. Qian, H. Che and J. Li, *J. Therm. Anal. Calorim.*, 2024, **149**, 2777–2787.
66 R. Wang, Y. Chen, Y. Liu, M. Ma, Z. Tong, X. Chen, Y. Bi, W. Huang, Z. Liao, S. Chen, X. Zhang and Q. Li, *Polym. Adv. Technol.*, 2021, **32**, 4700–4709.
67 X. Zhou, X. Mu, W. Cai, J. Wang, F. Chu, Z. Xu, L. Song, W. Xing and Y. Hu, *ACS Appl. Mater. Interfaces*, 2019, **11**, 41736–41749.
68 L. Sang, Y. Cheng, R. Yang, J. Li, Q. Kong and J. Zhang, *J. Therm. Anal. Calorim.*, 2020, **144**, 51–59.
69 B. Hou, K. Song, Z. Ur Rehman, T. Song, T. Lin, W. Zhang, Y.-T. Pan and R. Yang, *ACS Appl. Mater. Interfaces*, 2022, **14**, 14805–14816.
70 J. Zhang, Z. Li, Z.-B. Shao, L. Zhang and D.-Y. Wang, *Chem. Eng. J.*, 2020, **400**, 125942.
71 C. Chen, B. Wang, G. Xiao, M. Cao, F. Zhong, Z. Yang, J. Zhou, M. Wang and R. Zou, *Constr. Build. Mater.*, 2023, **394**, 132258.
72 X. Liu, P. Guo, B. Zhang and J. Mu, *Colloids Surf.*, 2023, **671**, 131625.
73 B. Hou, X. Song, K. Song, Z. Geng, Y.-T. Pan, P. Song and R. Yang, *J. Colloid Interface Sci.*, 2024, **654**, 235–245.
74 H. Wang, X. Li, F. Su, J. Xie, Y. Xin, W. Zhang, C. Liu, D. Yao and Y. Zheng, *ACS Omega*, 2022, **7**, 21664–21674.
75 K. Song, X. Bi, C. Yu, Y.-T. Pan, P. Xiao, J. Wang, J.-I. Song, J. He and R. Yang, *ACS Appl. Mater. Interfaces*, 2024, **16**, 15227–15241.
76 J. Zhang, Z. Li, L. Zhang, Y. Yang and D.-Y. Wang, *ACS Sustainable Chem. Eng.*, 2019, **8**, 994–1003.
77 J. Zhang, Z. Li, G.-Z. Yin and D.-Y. Wang, *Compos. Commun.*, 2021, **23**, 100594.
78 S.-L. Badea and V.-C. Niculescu, *Materials*, 2022, **15**, 3850.
79 X. Song, Q. Li, Z. Han, B. Hou, Y.-T. Pan, Z. Geng, J. Zhang, L. Haurie Ibarra and R. Yang, *J. Colloid Interface Sci.*, 2024, **667**, 223–236.
80 Y.-T. Pan, L. Zhang, X. Zhao and D.-Y. Wang, *Chem. Sci.*, 2017, **8**, 3399–3409.
81 M. Xue, R. Qin, C. Peng, L. Xia, Y. Xu, W. Luo, G. Chen, B. Zeng, X. Liu and L. Dai, *Compos. Commun.*, 2024, **46**, 101821.
82 Y. Wei, M. Wang, W. Qi and Z. He, *Process Saf. Environ. Prot.*, 2022, **163**, 636–644.
83 B. Tu, K. Zhou, Q. Zhou, K. Gong and D. Hu, *RSC Adv.*, 2021, **11**, 9942–9954.
84 K. Song, K. Zhang, X. Bi, B. Hou, Y.-T. Pan, X. Li, J. He and R. Yang, *J. Mater. Chem. A*, 2024, DOI: **10.1039/d4ta04677c**.
85 N. Habibi, S. Faraji and A. Pourjavadi, *Colloids Surf.*, 2023, **676**, 132186.
86 J. Cao, Y.-T. Pan, H. Vahabi, J.-I. Song, P. Song, D.-Y. Wang and R. Yang, *Mater. Today Chem.*, 2024, **37**, 102015.
87 Z. Han, W. Zhang, X. Song, H. Vahabi, Y.-T. Pan, W. Zhang and R. Yang, *Chem. Eng. J.*, 2023, **474**, 145682.